Contents lists available at ScienceDirect

Extreme Mechanics Letters

A new model based on the in-plane deformation for the conformal piezoelectric systems for characterization of soft tissue modulus

Hongyu Zhao [a,b], Canan Dagdeviren [c], Guodong Liu [a,b], Peng Cao [d], Jianru Wang [e], Baolin Sha [f], Guosheng Wang [g], Jingqiang Cui [g], Yewang Su [a,b,h,*]

[a] State Key Laboratory of Nonlinear Mechanics, Institute of Mechanics, Chinese Academy of Sciences, Beijing 100190, China
[b] School of Engineering Science, University of Chinese Academy of Sciences, Beijing 100049, China
[c] Media Lab, Massachusetts Institute of Technology, Cambridge, MA 02139, USA
[d] Faculty of Architecture,Civil and transportation Engineering, Beijing University of Technology, Beijing 100124, China
[e] Xi'an Aerospace Propulsion Technology Institute, Xi'an 710025, China
[f] The 41st Institute of the Fourth Academy of CASC, Xi'an 710025, China
[g] Henan Key Laboratory of Medical Polymer Materials Technology and Application, Tuoren Medical Device Research & Development Institute Co., Ltd., Tuoren Health Technology Industrial Park, Changyuan County, Henan 453000, China
[h] State Key Laboratory of Acoustics, Institute of Acoustics, Chinese Academy of Sciences, Beijing 100190, China

ARTICLE INFO

ABSTRACT

Mechanical assessment of the human skin is critically important for clinical diagnosis and treatment of disease. Past works developed a conformal piezoelectric system (CPS) that enables the noninvasive *in vivo* measurement of the elasticity modulus of the skin, and a mechanical model based on the mechanism of out-of-plane extension of the capacitor-type structures. Here, we present a new theoretical model that is established based on the mechanism of the in-plane deformation. The study on both the free-standing CPS and the CPS mounting to the polydimethylsiloxane (PDMS) target substrates verified the universality of the new model. The experimental and theoretical results consistently show that the output voltage of the first sensor approximately linearly increases with the increase of not only the applied voltage but also the modulus of the PDMS. The optimal usage mode of the CPS, in which the voltage is applied to all actuators simultaneously, is proposed for the measurement of the elastic modulus of target substrates such as skin.

The essential functions of human skin include protecting the inner viscera and tissue constituents from environmental hazards, pathogens and toxins, controlling the water, electrolytes and other biochemical mediators, sensing the physical stimuli such as force, heat, electricity, etc [1,2]. On the other hand, the basic physical properties of human skins under various conditions, are capable of reflecting the pathophysiologic conditions [3], predicting reactions to exogenous substances and environmental factors [4,5], facilitating the mechanisms associated with growth, repair and ageing, and evaluating the effectiveness of cosmetic products [5–9]. Particularly, the disorders such as scleroderma, Ehlers–Danlos syndrome, psoriasis, eczema, melanoma, and other cutaneous pathologies, involve changes of the elastic modulus of the skin [10–13].

Our preceding work (Nature Materials, 14 (2015) 728–736) presented a conformal piezoelectric system (CPS) that enables

the noninvasive *in vivo* measurement of the elastic modulus of the skin, [14] as shown in Fig. 1a-c. The CPS (Fig. 1d&e) consists of seven elongated piezoelectric actuators (lateral dimensions $w_a = 200$ μm, $L_a = 1000$ μm), six piezoelectric sensors (lateral dimensions $w_s = 100$ μm, $L_s = 500$ μm) with smaller sizes and stretchable electronic interconnects, mounted on the elastomer substrate (Ecoflex, thickness 20 μm, Young's modulus 60 kPa, Poisson's ratio 0.49). The spacing between a pair of sensors and actuators is $w_{gap} = 150$ μm (See SI for the detailed layouts). Each actuator or sensor is a capacitor-type structure incorporating a layer of piezoelectric material (lead zirconate titanate (PZT), 500 nm thick) between bottom (Ti/Pt, 20 nm/300 nm) and top (Cr/Au, 10 nm/200 nm) electrodes, with encapsulation layers of polyimide (PI, 1.2 μm thick for the bottom and 2.4 μm thick for the top). Here, the piezoelectric material is polarized along the thickness direction. Multiple actuators and sensors result much stronger detected response of sensors and prevent failure of the experiment caused by any capacitor-type structure damage. With the CPS conformally mounted on a target substrate, such as human skin, application of a sinusoidally varying voltage to selected actuator yields mechanical motions of the PZT and the entire

* Corresponding author at: State Key Laboratory of Nonlinear Mechanics, Institute of Mechanics, Chinese Academy of Sciences, Beijing 100190, China.
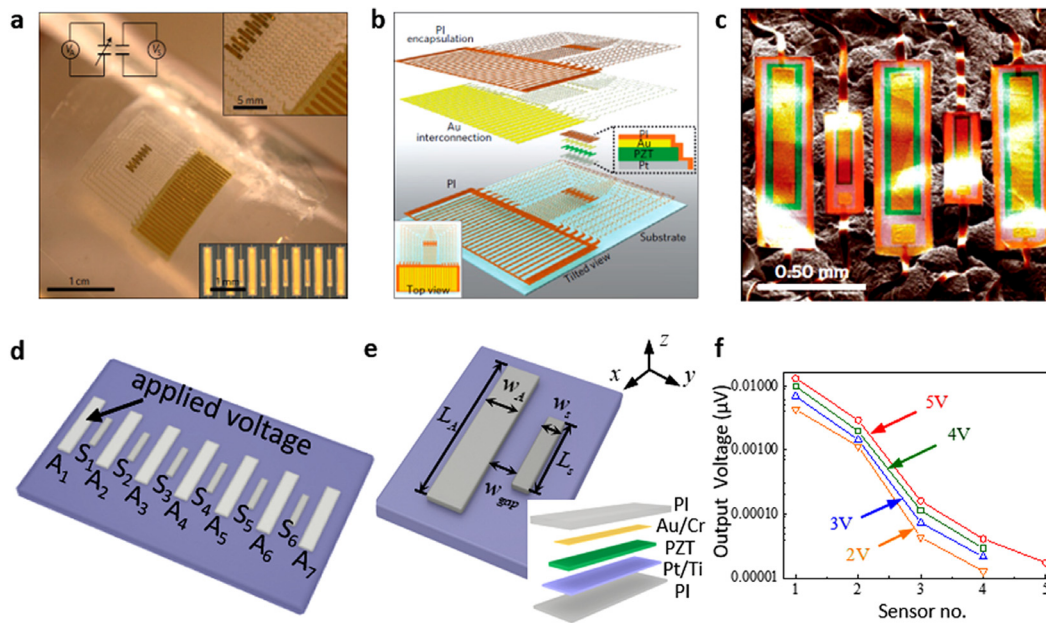*E-mail address:* yewangsu@imech.ac.cn (Y. Su).

Fig. 1. Conformal piezoelectric systems for measurements of skin modulus with ultrathin, stretchable structures of mechanical actuators and sensors. (a) Photograph of the CPS. Optical microscope image of the serpentine interconnects (upper-right inset), the actuator and sensor arrays with ultrathin structure (lower-right inset), and an electrical circuit diagram of actuators and sensors (upper-left inset) (with permissions). (b) The schematic diagrams of the CPS, which consist of piezoelectric material (PZT), bottom (Pt/Ti) and top (Cr/Au) electrodes and encapsulation layers of PI, supported by a thin elastomer substrate. A top view at the lower-left inset (with permissions). (c) SEM image of actuator and sensor on an artificial skin sample (with permissions). (d) Schematic diagram of the experimental test, in which CPS is freestanding without mounting to any target substrate. (e) Different dimensions of each layer for the actuators or sensors are simplified to uniform in-plane dimensions. (f) The output voltages for each of the different sensors (that is, sensor no. 1, no. 2, and so on) under different applied voltages when the CPS is freestanding without mounting to the skin.

capacitor-type structure, which would be transferred to nearby sensors through the physically contacted target substrate and the elastomer substrate of the CPS. The elastic modulus of the target substrate can be determined by the relationship between the detected voltage response of sensors and the applied voltage to the selected actuator. The underlying mechanism of deformation transfer and the quantitative theoretical model are crucial for the feasibility and accuracy of the modulus measurement via the CPS. In the mechanism analysis of the past work, the entire model coupling the CPS and the target substrate is treated as interfacial cracks, in which the effects of the interfacial shear strain/stress were neglected [14]. Application of the external voltage to a selected capacitor-type actuator induces the out-of-plane extension, which is transferred, with degenerative amplitude, to nearby sensors through the coupling out-of-plane extension of the target substrate and elastomer substrate. The detected response of nearby sensors determinates the elastic modulus of the target substrate.

Recently, a further experimental test is conducted to investigate the mechanism of the deformation transfer of the CPS. In the experiments, the external voltage is applied to actuator A_1, as shown in Fig. 1d, while the CPS is freestanding without mounting to any target substrate. According to our proceeding theory, the detected response of nearby sensors would vanish, because the out-of-plane extension of the actuator cannot be transferred to anywhere without the coupling out-of-plane extension of the skin and the elastomer substrate. However, a similar response trend of the case where the CPS is mounted on the low moduli PDMS, is captured (Fig. 1f). The detected output voltages decay in an approximately exponential fashion with the increase of the distance between the sensor and the active actuator. This paper aims to investigate the indepth mechanism of the deformation transfer and propose a new theoretical model for the modulus measurement, which is universal for diverse tests.

1. Results

Evidence for the mechanism that the in-plane lengthwise shear strain dominates the deformation transfer. According to the recent experimental results (Fig. 1f), it can be deduced that deformation transfer among the actuator and the sensors through the skin and the elastomer substrate is based on the mechanism of in-plane deformation. In this new model, the mechanism of in-plane deformation dominates the deformation transfer, which includes the lengthwise and widthwise extensions of the PZT of the actuator, the shear strains of the elastomer substrate, as well as the corresponding deformation of the sensors. Regarding the direction of the deformation components, finite element analysis (FEA) coupling both mechanical and electric fields are conducted for the three models as shown in Fig. 2a-c. The solid element was adopted for the elastomer substrate and the PZT layer (the material parameters are shown in Note 1). The other layers of the actuator and sensor were treated as a linear elastic material and the shell element was adopted. Three different types of constrain conditions are applied to the interface between the actuators/sensors and the elastomer substrate. The "Tie" constraint is adopted in Fig. 2a to simulate the deformation transfer along both the lengthwise and widthwise directions. The "Coupling" constraint is adopted in Fig. 2b&c to simulate the deformation transfer along only the widthwise or the lengthwise direction (See SI for the detail). The directions of the arrows represent the directions of the interfacial shear stress which are opposite on the actuators/sensors and the elastomer substrate. In Fig. 2a, the deformation of the actuator A_1 can be transferred to the elastomer substrate along both the lengthwise and widthwise directions, while in Fig. 2b or in Fig. 2c, the deformation transfer takes effects along only the widthwise or the lengthwise direction, respectively. The FEA shows that the results of the cases of both directions and lengthwise direction approach that of the
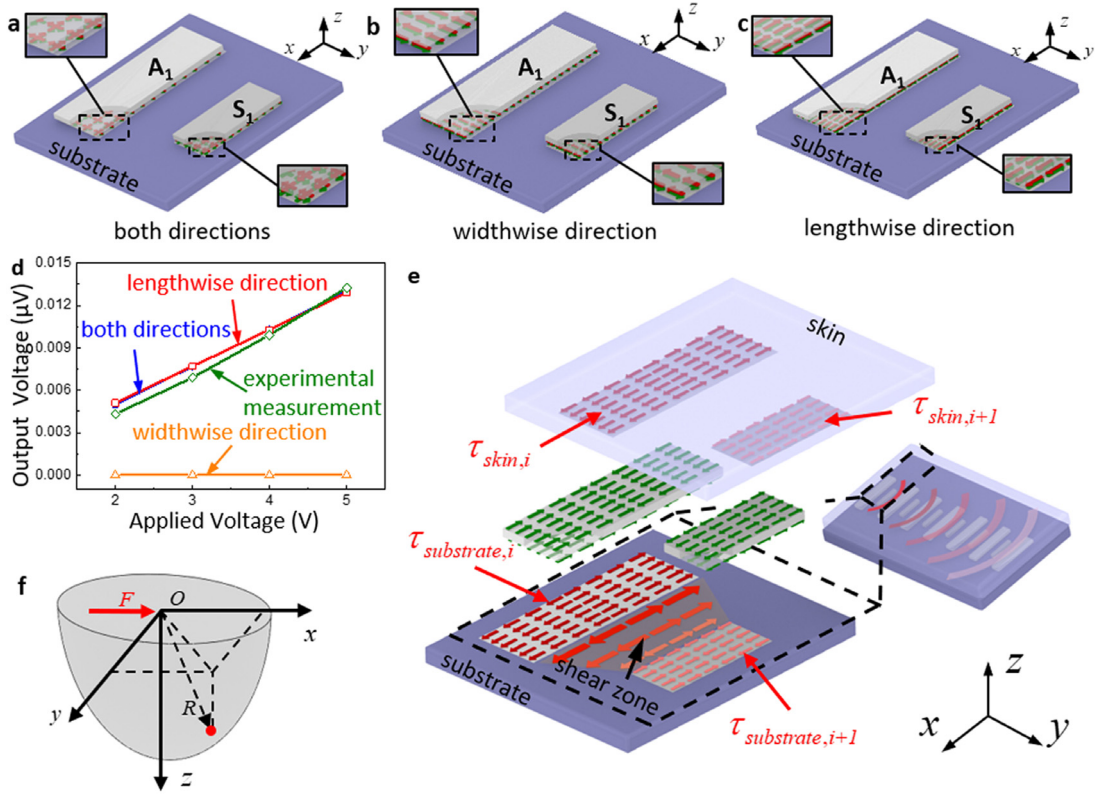
Fig. 2. Three models for the mechanism of the deformation transfer for considering shear stress along (a) both the lengthwise and widthwise directions, (b) only the widthwise direction (y-direction) (c) only the lengthwise direction (x-direction). The shear stress on the capacitor-type structure and the elastomer substrate is indicated by red and green arrows. (d) Numerical results for three models and experimental results of the first sensor under different applied voltages. (e) The model for the mechanism of the deformation transfer. (f) The model for the Cerruti problem.

experimental test, while the response of the case of widthwise direction is much smaller by 4 orders of magnitude, as depicted in Fig. 2d. Obviously, the dominated mechanism is that the in-plane lengthwise extension of the actuator is transferred, via the shear strain of the elastomer substrate, to the in-plane lengthwise extension of the nearby sensors (Fig. 2e).

The new theoretical model. The model for the mechanism of the deformation transfer is shown in Fig. 2e. Both actuators and sensors are capacitor-type structures incorporating a layer of PZT between bottom and top electrodes, with encapsulation layers of PI. They have the same architectural design along the thickness direction but different in-plane sizes. Therefore, the universal serial number i from 1 to 13 for all the capacitor-type structures is used in the following analysis. L_i and w_i denote the length and the width of each capacitor-type structure, respectively. With the applied voltage $V_{app,i}$, the ith capacitor-type structure (the actuator) deforms along the lengthwise direction because of the inverse piezoelectric effect, subsequently yields the shear strain of the surrounding elastomer substrate and the skin/calibration materials, and results the lengthwise deformation of the nearby capacitor-type structures (sensors and actuators that are without applied voltage). The output voltage of the sensors can be detected to reflect the modulus of the skin/calibration materials. Here, the new analytic model aims to give the relation between the output voltages of the sensors and the applied voltage of the actuator in terms of the elastic modulus of the skin.

The capacitor-type structure consisting of multilayers (PI/Ti/ Pt/PZT/Cr/Au/PI) is analyzed firstly for the actuators and sensors. For the PZT layer of the ith capacitor-type structure, the condition of traction free along the thickness direction, the polarization direction and the simple model of applied voltage give the stress $\sigma_{33,i} = 0$ and the electric field intensity $E_{1,i} = E_{2,i} = 0$,

which reduce the linear constitutive relations of the piezoelectric material PZT to

$$
\begin{cases}
\sigma_{11,i} = c_{11}\varepsilon_{11,i} + c_{12}\varepsilon_{22,i} + c_{13}\varepsilon_{33,i} - e_{31}E_{3,i} \\
\sigma_{22,i} = c_{12}\varepsilon_{11,i} + c_{11}\varepsilon_{22,i} + c_{13}\varepsilon_{33,i} - e_{31}E_{3,i} \\
0 = c_{13}\varepsilon_{11,i} + c_{13}\varepsilon_{22,i} + c_{33}\varepsilon_{33,i} - e_{33}E_{3,i} \\
D_{3,i} = e_{31}\varepsilon_{11,i} + e_{31}\varepsilon_{22,i} + e_{33}\varepsilon_{33,i} + k_{33}E_{3,i}
\end{cases}
\tag{1}
$$

Here, $\sigma_{pq,i}$ and $\varepsilon_{pq,i}$ $(p, q = 1, 2, 3)$ are the components of stress tensor and strain tensor, $E_{p,i}$ and $D_{p,i}$ $(p = 1, 2, 3)$ are the component of electric field intensity and electric displacement vector, c_{pq}, e_{pq}, k_{pq} $(p, q = 1, 2, 3)$ are elastic stiffness constant, piezoelectric stress constant and dielectric coefficient, respectively. For the entire capacitor-type structure with slender aspect, the balance among the multilayers along the lengthwise direction, together with the condition of traction free along the widthwise direction, yield

$$
\begin{cases}
\varepsilon_{11,i} = aE_{3,i} + bf_i \\
\varepsilon_{22,i} = aE_{3,i} - cf_i \\
D_{3,i} = \bar{e}\left(\varepsilon_{11,i} + \varepsilon_{22,i}\right) + \bar{k}E_{3,i}
\end{cases}
\tag{2}
$$

where a, b and c are given in Box I

$\bar{e} = e_{31} - \frac{c_{13}e_{33}}{c_{33}}$ and $\bar{k} = k_{33} + \frac{e_{33}^2}{c_{33}}$ are the related coefficients. Here, f_i is the resultant force per unit width at the ends of the ith slender capacitor-type structure along the lengthwise direction, t_{PZT} is the thickness of the PZT layer, t_n, $\bar{E}_n$ and ν_n are thickness, plane-strain effective modulus and Passion's ratio for each layer, respectively (See SI for the detail). For the actuator, the relation $V_{app,i} = E_{3,i}t_{PZT}$ and $u_i = \varepsilon_{11,i}L_i/2$, together with the first equation

$$a = \frac{t_{PZT} \left(c_{33}e_{31} - c_{13}e_{33}\right)/c_{33}}{\left[\sum_{n=1\sim3,\,5\sim7} \overline{E}_n t_n + t_{PZT}\left(c_{11}c_{33} - c_{13}^2\right)/c_{33}\right] + \left[\sum_{n=1\sim3,\,5\sim7} \nu_n \overline{E}_n t_n + t_{PZT}\left(c_{12}c_{33} - c_{13}^2\right)/c_{33}\right]},$$

$$b = \frac{\sum_{n=1\sim3,\,5\sim7} \overline{E}_n t_n + t_{PZT}\left(c_{11}c_{33} - c_{13}^2\right)/c_{33}}{\left[\sum_{n=1\sim3,\,5\sim7} \overline{E}_n t_n + t_{PZT}\left(c_{11}c_{33} - c_{13}^2\right)/c_{33}\right]^2 - \left[\sum_{n=1\sim3,\,5\sim7} \nu_n \overline{E}_n t_n + t_{PZT}\left(c_{12}c_{33} - c_{13}^2\right)/c_{33}\right]^2},$$

$$c = \frac{\sum_{n=1\sim3,\,5\sim7} \nu_n \overline{E}_n t_n + t_{PZT}\left(c_{12}c_{33} - c_{13}^2\right)/c_{33}}{\left[\sum_{n=1\sim3,\,5\sim7} \overline{E}_n t_n + t_{PZT}\left(c_{11}c_{33} - c_{13}^2\right)/c_{33}\right]^2 - \left[\sum_{n=1\sim3,\,5\sim7} \nu_n \overline{E}_n t_n + t_{PZT}\left(c_{12}c_{33} - c_{13}^2\right)/c_{33}\right]^2},$$

Box I.

of Eq. (2) give

$$\frac{2u_i}{L_i} = a\frac{V_{app,i}}{t_{PZT}} + bf_i, \tag{3}$$

where $V_{app,i}$, L_i and u_i are the applied voltage to the ith capacitor-type structure (the actuator), the length of the ith capacitor-type structure and the displacement at the end. For each sensor and each actuator that is without applied voltage, the condition of zero electric displacement $D_{3,i} = 0$, the relation $V_{out,i} = E_{3,i}t_{PZT}$ and $u_i = \varepsilon_{11,i}L_i/2$, together with Eq. (2) result the relation

$$\frac{2u_i}{L_i} = \frac{\overline{e}a(b+c) + \overline{k}b}{2\overline{e}a + \overline{k}}f_i, \tag{4}$$

and the output voltage

$$V_{out,i} = -\frac{\overline{e}t_{PZT}(b-c)}{2\overline{e}a + \overline{k}}f_i, \tag{5}$$

which can be detected by the oscilloscope.

Regarding the deformation of the elastomer substrate, it is considered as a semispace elastomer subjected to distributed shear stress at the location of the actuators and sensors along the lengthwise direction, as shown in Fig. 2e&f. For simplification, the shear stress is assumed to be uniform at the location of each actuator or sensor. Because of the symmetricity, the directions of shear stress along the lengthwise direction are opposite on either side of the axis of symmetry, which are denoted by opposite arrows in Fig. 2e. To obtain the effect of the shear force on the deformation of the elastomer substrate, the solution of the Cerruti problem [15] is introduced, as shown in Fig. 2f, which is the problem of a semispace elastomer subjected to a tangential concentrated force. Using this classic solution, integration of the effect of the distributed shear stress on the displacement over all the locations of the sensors and actuators, gives the displacement at the end of the sensor or the actuator as

$$u_{substrate,i} = \sum_{j=1}^{13} \frac{(1 + \nu_{substrate})\,\tau_{substrate,j}}{\pi E_{substrate}}$$
$$\times \left\{ \begin{array}{l} \int_{y=-w_j/2-(j-i)d}^{w_j/2-(j-i)d} \int_{x=(L_i-L_j)/2}^{L_i/2} \left[\frac{1 - \nu_{substrate}}{\left(x^2 + y^2\right)^{\frac{1}{2}}} + \frac{\nu_{substrate}x^2}{\left(x^2 + y^2\right)^{\frac{3}{2}}} \right] \\ \quad \times dxdy \\ - \int_{y=-w_j/2-(j-i)d}^{w_j/2-(j-i)d} \int_{x=L_i/2}^{(L_i+L_j)/2} \left[\frac{1 - \nu_{substrate}}{\left(x^2 + y^2\right)^{\frac{1}{2}}} + \frac{\nu_{substrate}x^2}{\left(x^2 + y^2\right)^{\frac{3}{2}}} \right] \\ \quad \times dxdy \end{array} \right\}, \tag{6}$$

where $E_{substrate}$, $\nu_{substrate}$ are the elastic modulus and the Passion's ratio of the elastomer substrate, $\tau_{substrate,j}$ denotes the shear stress

on the elastomer substrate subjected by the jth capacitor-type structure, w_i, w_j, L_i, L_j are the width and length of the ith and the jth capacitor-type structure, d is the spacing distance between the centers of adjacent capacitor-type structures, respectively (See SI for the detail). The above analysis also holds for the skin or the calibration materials, which yields

$$u_{skin,i} = \sum_{j=1}^{13} \frac{(1 + \nu_{skin})\,\tau_{skin,j}}{\pi E_{skin}}$$
$$\times \left\{ \begin{array}{l} \int_{y=-w_j/2-(j-i)d}^{w_j/2-(j-i)d} \int_{x=(L_i-L_j)/2}^{L_i/2} \left[\frac{1 - \nu_{skin}}{\left(x^2 + y^2\right)^{\frac{1}{2}}} + \frac{\nu_{skin}x^2}{\left(x^2 + y^2\right)^{\frac{3}{2}}} \right] \\ \quad \times dxdy \\ - \int_{y=-w_j/2-(j-i)d}^{w_j/2-(j-i)d} \int_{x=L_i/2}^{(L_i+L_j)/2} \left[\frac{1 - \nu_{skin}}{\left(x^2 + y^2\right)^{\frac{1}{2}}} + \frac{\nu_{skin}x^2}{\left(x^2 + y^2\right)^{\frac{3}{2}}} \right] \\ \quad \times dxdy \end{array} \right\}, \tag{7}$$

where E_{skin}, ν_{skin} are the elastic modulus and the Passion's ratio of the skin, $\tau_{skin,j}$ denotes the shear stress on the skin subjected by the jth capacitor-type structure, respectively.

For the mechanical coupling among the actuators, sensors, elastomer substrate and skin, the displacements, the shear stress and the resultant force per unit width are required to satisfy

$$\begin{cases} u_i = u_{substrate,i} = u_{skin,i} \\ f_i = \frac{L_i}{4}\left(\tau_{substrate,i} + \tau_{skin,i}\right) \end{cases}, \tag{8}$$

instead of accurately agreement everywhere, which involves the concept of average without loss of generality. The solution of the linear Eqs. (3)–(8), which can be obtained by the program package MATLAB [16] with substituted geometric and material parameters, gives the quantitative relationships among the output voltages, the applied voltage and skin modulus.

The comparison of the experimental and theoretical results. For the experimental test of the freestanding CPS without mounting to any target substrate, the effect of the target substrate can be neglected in the above analysis. Eq. (8) becomes

$$\begin{cases} u_i = u_{substrate,i} \\ f_i = \frac{L_i}{4}\tau_{substrate,i} \end{cases}, \tag{9}$$

which, together with Eqs. (3)–(6), give the quantitative relationships among the output voltages, the applied voltage and the modulus of the target substrate. Fig. 3a&b show that the theoretical predictions agree very well with the experimental results, for the applied voltage from 1~5V to the actuator A_1. The output voltage decays in an approximately exponential fashion with the
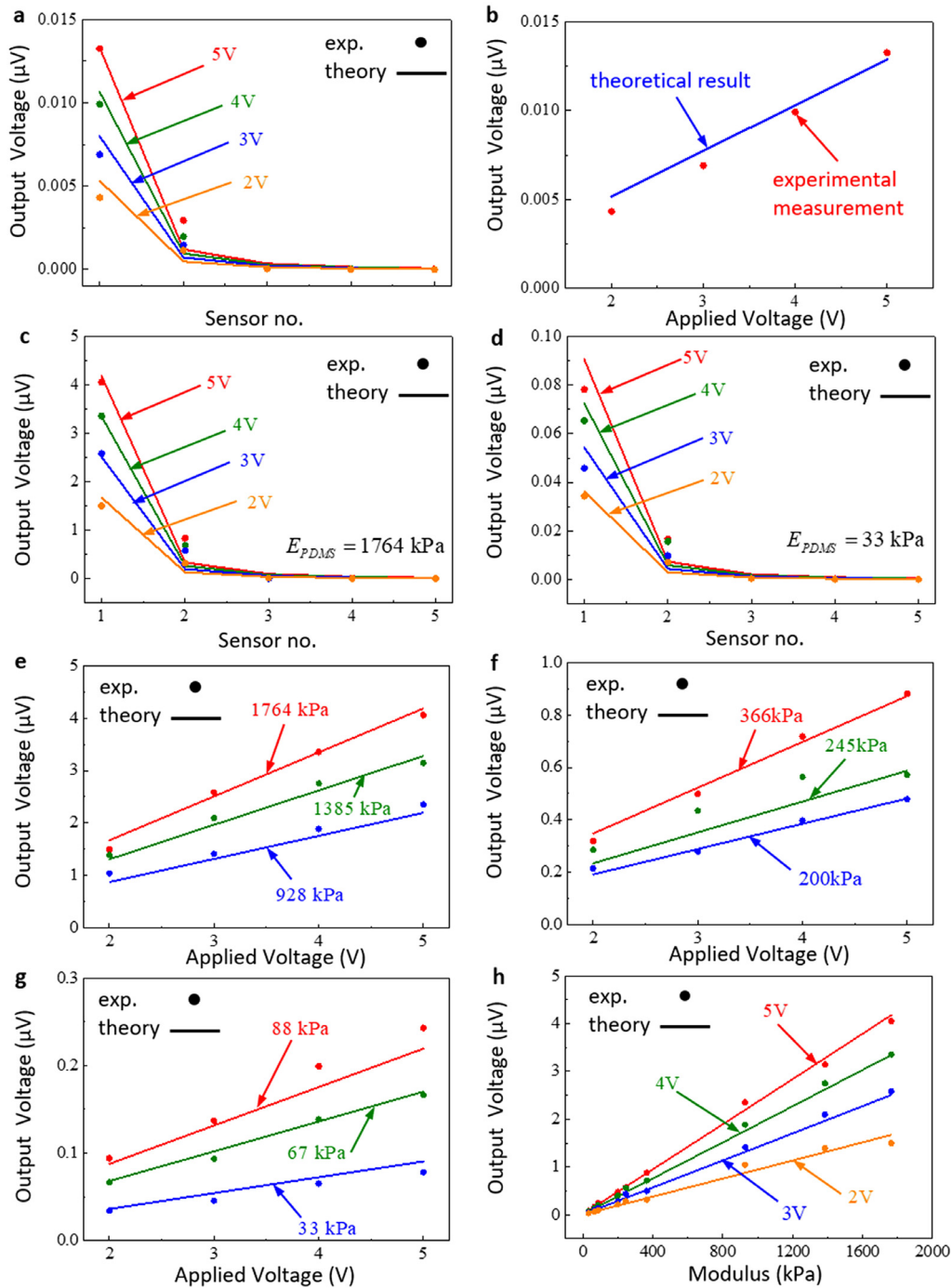
Fig. 3. (a) Theoretical and experimental results for the free-standing CPS without mounting to the skin under different applied voltages. (b) Theoretical and experimental results of the first sensor under different applied voltages. Output voltages for each of the different sensors in the array (that is, sensor no. 1, no. 2, and so on) measured during use with two kinds of PDMS substrates with different modulus: (c) $E_{PDMS} = 1764$ kPa, (d) $E_{PDMS} = 33$ kPa. ((e)–(g)) Output voltage of the first sensor (the sensor adjacent to the active actuator) as a function of applied voltage, measured on nine different PDMS substrates with known moduli. (h) Output voltage from the first sensor as a function of the modulus of the PDMS under four applied voltages.

increase of the distance between the sensor and the actuator, while increases with the increase of the applied voltage (Fig. 3a). The reason for the small strain response is that the freestanding CPS without mounting to any target substrate yields much small deformation of the surrounding elastomer substrate, and results much small detected voltage response of sensors. The voltage amplitude of the first sensor (the sensor adjacent to the active actuator), which is much larger than others, varies linearly with the applied voltage, as shown in Fig. 3b.

The theoretical model consisting of both the CPS and the target substrate is validated by experiments that involve a set of calibration materials of polydimethylsiloxane (PDMS) with a range of elastic modulus (33 kPa and 1764 kPa in Fig. 3c&d) reasonably relevant to human skin (separately evaluated using a dynamic mechanical analyzer). The output voltage for each sensor of the CPS is shown in Fig. 3c-d, while different voltages are applied to the first actuator. It indicates good agreement between theoretical results (calculate from Eqs. (3)–(7), Eq. (9))
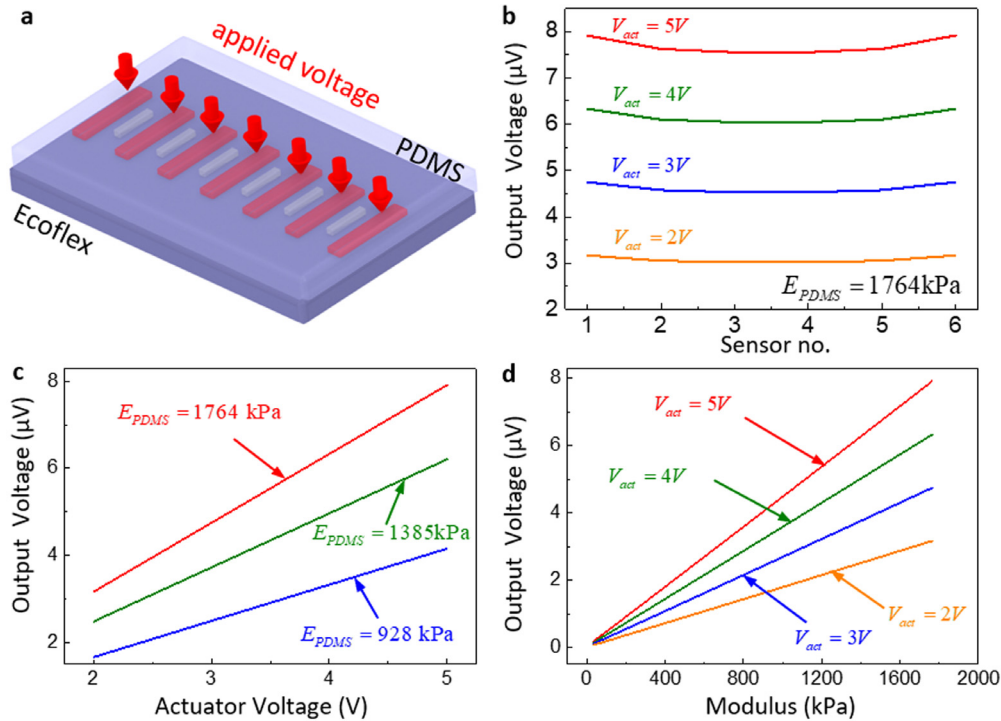
Fig. 4. (a) Schematic illustration for all actuators subjected to the applied voltage. (b) Prediction of the output voltages under different applied voltages, measured during use with PDMS substrates (E_{PDMS} = 1764 kPa). Output voltage of the first sensor varies linearly with (c) the applied voltages and approximately linearly with d) the elastic modulus of PDMS.

and experimental results. With the increase of the distance between the sensor and the active actuator, the output voltage decreases exponentially. The output voltage from the first sensor (the sensor adjacent to the active actuator) is much larger than the output voltage from the other sensors by several orders of magnitude. Therefore, the output voltage of the first sensor is used to evaluate the relationship between the elastic modulus and the output voltage of the sensors. Focusing on the output voltage of the first sensor, more experiments were conducted with different PDMS with moduli of 1764, 1385, 928, 366, 245, 200, 88, 67 and 33 kPa, respectively, as shown in Fig. 3e∼h. The experimental and theoretical results consistently show that the output voltage of the first sensor approximately linearly increases with the increase of not only the applied voltage but also the modulus of the calibration material PDMS. The average errors of the output voltage of the first sensor are 2.86%, 1.08%, 1.65%, 0.24%, 0.69%, 0.14%, 2.40%, 0.57%, 12.70% for the different PDMS with moduli of 1764, 1385, 928, 366, 245, 200, 88, 67 and 33 kPa in different applied voltages. The average errors of the output voltage of the first sensor are 1.28%, 4.15%, 0.31, 3.12% for different applied voltages of 5 V, 4 V, 3 V, 2 V with different PDMS with moduli. It indicates that there is no obvious relationship between the average errors and the elastic modulus or applied voltages. Although there is a small discrepancy between the theoretical and experimental values, the variation in the elastic modulus of dozens of kPa can be obtained by the combination of CPS and the theoretical model. Therefore, it is sufficient for the variation measurements of the skin in MPa orders.

The above study on the free-standing CPS and the CPS mounting to the calibration target material (PDMS) verified the universality of the new theoretical model. In the previous experiments, the voltage was applied to only the first actuator. Here, we

propose to apply the voltage to all the actuators simultaneously (Fig. 4a). Based on the theoretical analysis in this section, the prediction with all actuators subjected to applied voltages is given in Fig. 4b∼d. Under the same applied voltage to the actuators, the output voltages from each sensor have similar magnitude trend, as shown in Fig. 4b, which are stronger than those of the previous mode, in which an individual actuator is applied voltage at a time. A strong voltage response is beneficial to voltage detection. Meanwhile, we can obtain the elastic modulus of skin from the output voltage of any sensors. It prevents failure of the experiment caused by any sensor damage. The same regularity emerges that the amplitudes of sensor voltages vary approximately linearly with the applied voltage (Fig. 4c) and with the elastic modulus of the calibration material PDMS (Fig. 4d). Thus, this usage mode of the CPS is an effective method to measure the elastic modulus of skin. What needs to be pointed out is that the relationship between the output voltage and the elastic modulus of skin needs to be calibrated by using exact experiment results during the use of the mode where a voltage is applied to all actuators.

2. Conclusions

Mechanical characterization of the human skin is critically important for clinical diagnosis and treatment of disease. Following our preceding work on the CPS that enables the noninvasive *in vivo* measurement of the elasticity modulus of the skin, here, further experimental study on the free-standing CPS without mounting to any target substrate and FEA results revealed that the deformation transfer is based on both the mechanism of in-plane lengthwise extension of the actuator and the shear strain of the elastomer substrate (and the skin). A new theoretical model is

established, the universality of which is verified via the study on both the free-standing CPS and the CPS mounting to the PDMS. The experimental and theoretical results consistently show that the output voltage of the first sensor approximately linearly increases with the increase of not only the applied voltage but also the elastic modulus of the PDMS. For optimization, the voltage is applied to all the actuators instead of only the first actuator, so that stronger output voltage can be obtained from all the sensors. The combination of the CPS and the present theoretical model provides an effective new approach for characterization of soft tissue biomechanics.

CRediT authorship contribution statement

Hongyu Zhao: Derived the theory, Numerical simulation, Discussed all the data, Prepared the manuscript. **Canan Dagdeviren:** Carried out the experiment. **Guodong Liu:** Numerical simulation. **Peng Cao:** Discussed all the data, Prepared the manuscript. **Jianru Wang:** Discussed all the data, Prepared the manuscript. **Baolin Sha:** Discussed all the data, Prepared the manuscript. **Guosheng Wang:** Discussed all the data, Prepared the manuscript. **Jingqiang Cui:** Discussed all the data, Prepared the manuscript. **Yewang Su:** Conceived the concept, Derived the theory, Discussed all the data, Prepared the manuscript, Supervision.

Declaration of competing interest

The authors declare that they have no known competing financial interests or personal relationships that could have appeared to influence the work reported in this paper.

Acknowledgments

Appendix A. Supplementary data

Supplementary material related to this article can be found online at https://doi.org/10.1016/j.eml.2022.101801. Supporting Information is available from the Wiley Online Library or from the author.

References

[1] P.M. Elias, Stratum corneum defensive functions: An integrated view, J. Invest. Dermatol. 20 (2005) 183–200.
[2] N. Charkoudian, Skin blood flow in adult human thermoregulation: How it works, when it does not, and why, Mayo Clin. Proc. 78 (2003) 603–612.
[3] M.J. Paszek, N. Zahir, K.R. Johnson, J.N. Lakins, G.I. Rozenberg, A. Gefen, C.A. Reinhart-King, S.S. Margulies, M. Dembo, D. Boettiger, D.A. Hammer, V.M. Weaver, Tensional homeostasis and the malignant phenotype, Cancer Cell 8 (2005) 241–254.
[4] S. Friberg, Micelles, microemulsions, liquid crystals, and the structure of stratum corneum lipids, J. Soc. Cosmet. Chem. 41 (1990) 155–171.
[5] M.M. Rieger, D.E. Deem, Skin moisturizers. II. The effects of cosmetic ingredients on human stratum corneum, 25, 1974, pp. 253–262.
[6] N. Magnenat-Thalmann, P. Kalra, J.L. Leveque, R. Bazin, D. Batisse, B. Querleux, A computational skin model: fold and wrinkle formation, IEEE Trans. Inf. Technol. Biomed. 6 (2002) 317–323.
[7] D. Batisse, R. Bazin, T. Baldeweck, Influence of age on the wrinkling capacities of skin, 8, 2002, pp. 148–154.
[8] H. Alexander, T. Cook, Variations with age in the mechanical properties of human skin in vivo, J. Tissue Viability 16 (2006) 6–11.
[9] R. Grahame, P.J.L. Holt, The influence of ageing on the in vivo elasticity of human skin, Gerontology 15 (1969) 121–139.
[10] F. Hendriks, Mechanical Behaviour of Human Epidermal and Dermal Layers in Vivo, Technische Universiteitndhoven, 2005.
[11] A.B. Cua, K.P. Wilhelm, H.I. Maibach, Elastic properties of human skin: relation to age, sex, and anatomical region, Arch. Dermatol. Res. 282 (1990) 283–288.
[12] N. Kashibuchi, Y. Hirai, K. O'Goshi, H. Tagami, Three-dimensional analyses of individual corneocytes with atomic force microscope: morphological changes related to age, location and to the pathologic skin conditions, Skin Res. Technol. 8 (2002) 203–211.
[13] V. Lulevich, T. Zink, H.-Y. Chen, F.-T. Liu, G.-y. Liu, Cell mechanics using atomic force microscopy-based single-cell compression, Langmuir 22 (2006) 8151–8155.
[14] C. Dagdeviren, Y. Shi, P. Joe, R. Ghaffari, G. Balooch, K. Usgaonkar, O. Gur, P.L. Tran, J.R. Crosby, M. Meyer, Y. Su, R. Chad Webb, A.S. Tedesco, M.J. Slepian, Y. Huang, J.A. Rogers, Conformal piezoelectric systems for clinical and experimental characterization of soft tissue biomechanics, Nature Mater. 14 (2015) 728–736.
[15] P. Podio-Guidugli, A. Favata, The cerruti problem, in: Elasticity for Geotechnicians: A Modern Exposition of Kelvin, Boussinesq, Flamant, Cerruti, Melan, and Mindlin Problems, Springer International Publishing, Cham, 2014, pp. 149–157.
[16] M. Sordia, Program package MATLAB, 2012.